

# Surface Modification of Polyethylene by Remote dc Discharge Plasma Treatment

J. BEHNISCH, A. HOLLÄNDER, and H. ZIMMERMANN

Fraunhofer Einrichtung für Angewandte Polymerforschung, Kantstraße 55, D-O-1530 Teltow-Seehof, Germany

## SYNOPSIS

The surface modification of polyethylene in a remote nitrogen, oxygen, and hydrogen dc discharge plasma was investigated. In the case of the nitrogen plasma a strong correlation exists between the concentration of active nitrogen species, as detected by Langmuir probe measurements and plasma emission spectroscopy, and the time dependence of the polymer surface modification, as detected by contact-angle measurements. The obtained contact-angle data were interpreted in terms of the acid-base model for the interaction of the test liquid with the polymer surface. There was a great similarity in the functionalization of the polyethylene surfaces treated with nitrogen as well as with oxygen plasma, except in the initial stage, where in the former, mainly functional groups acting as electron acceptors were formed, whereas in the latter a sharp increase in the content of both electron donor as well as electron acceptor groups was detected. Thus, a determining influence of oxygen residues in the remote nitrogen plasma was indicated. The absence of such an effect in the case of the hydrogen plasma could result from direct quenching of reactive oxygen species and/or the chemical reduction of formed oxygen containing functionalities by hydrogen species. © 1993 John Wiley & Sons, Inc.

## INTRODUCTION

Low-pressure plasma treatment of polymers is a powerful tool to modify their surface properties by the introduction of different functional groups. However, its application in controlled surface engineering of advanced polymer materials is limited because of the chemical heterogeneity of the functionalized surfaces caused by the different reactive plasma species, such as free electrons, electronically excited atoms and molecules, radicals, ions, and radiation.

One possibility to improve the selectivity of the functionalization is to keep the polymer outside of the main discharge zone to avoid the uncontrolled cleavage of chemical bonds of the macromolecules by direct particle bombardment (sputtering) and to reduce the variety of reactive species by the different recombination reactions in the afterglow. Therefore, the nitrogen plasma treatment of polyethylene in a remote plasma reactor was introduced recently.<sup>1</sup>

In this work a special kind of a remote plasma reactor is used, where the sample is placed downstream behind the cathode of a dc glow discharge. Thus, "weak" plasma conditions should be realized allowing a more detailed investigation and control of the plasma/polymer interactions.

## EXPERIMENTAL

### Materials

Polyethylene (PE) films (Lupolen) were supplied by BASF. Before treatment the film was cleaned with 96% ethanol in a ultrasound cleaner for 5 min and dried for 1 h at 50°C in a vacuum oven.

### Plasma Treatment

A special kind of a remote plasma reactor was used, where the sample is located downstream behind the cathode (a steel grid) of a dc glow discharge (Fig. 1). The discharge voltage was 750 V and the resulting discharge current was 1.4 mA.

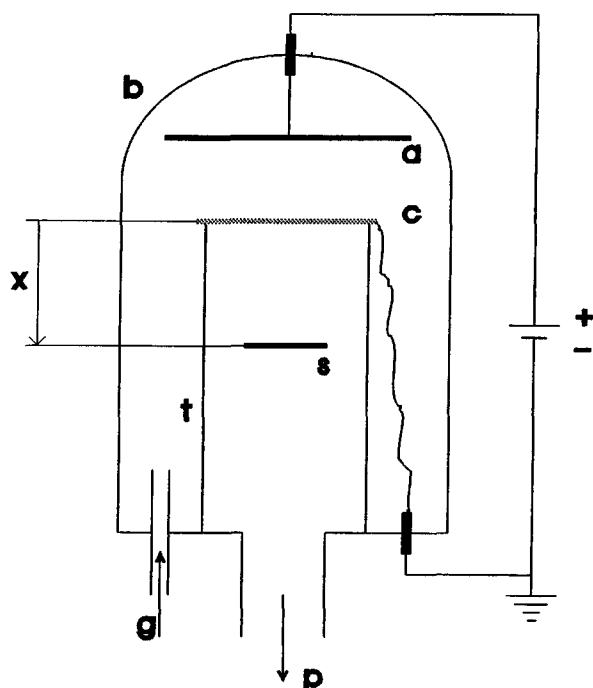


**Figure 1** Scheme of the plasma reactor used in this work: b, bell jar; a, anode; c, cathode; t, glass tube; g, gas inlet; p, pump; s, sample; x, distance behind the cathode.

After insertion of the sample the reactor was evacuated for 10 min to a base pressure of about 2 Pa using a rotary pump (Alcatel 2020A). Then, the gas flow controller (MKS 1959C) was turned on to its maximum (200 sccm) for 5 min before the process flow rate of 15 sccm was realized. The resulting pressure during the plasma treatment was 40 Pa. Oxygen, nitrogen (5.0), and hydrogen (5.0) (Linde AG, Berlin) were used as received.

### Plasma Diagnostics

For the determination of internal plasma parameters a Langmuir probe in the form of a metal sheet ( $4 \times 4 \text{ cm}^2$ ) was located in place of the sample. The probe was connected via a power supply and an ammeter to the grounded cathode.

The plasma emission was detected via a quartz fiber system by a 0.2 m monochromator (Verity Instruments).

### Contact Angle Measurements

The advancing and receding contact angles of the test liquids were determined by putting a 3–8-mm drop on the polymer film. The angles were measured at 295 K using a goniometer video system G40 (Krüss GmbH, Hamburg). The surface tension of

the test liquids was controlled by the Wilhelmi plate method using a tensiometer K12 (Krüss GmbH) using an annealed platinum plate. Test liquids were utilized: deionized water with a surface tension of  $\gamma = 72.8 \text{ mN/m}$ , formamide (Fluka, puriss. p.a.) with  $\gamma = 57.7 \text{ mN/m}$ , and tricresylphosphate (Fluka, pract., mixture of isomers) with  $\gamma = 41.4 \text{ mN/m}$ .

The measurements of the plasma-treated samples were performed immediately after removing from the reactor. The presented contact angles are averaged from at least two independent experimental runs and the deviation from the average is not greater than  $\pm 3^\circ$ . No changes of the contact angles during the time of measurement using all three test liquids (less than 30 min) were observed.

## RESULTS

### Nitrogen Plasma

#### Plasma Diagnostics

The Langmuir probe measurements presented in Figure 2 (where  $U_p$  and  $I_p$  are the probe voltage and the probe current, respectively) indicate a regular dependence of the internal plasma parameters on the position behind the cathode. The ion saturation current  $I_i^*$  [defined here as  $I_i^* = I_p(U_p = 0)$ ] and the floating potential  $U_f$  [ $U_f = U_p(I = 0)$ ] decreases with increasing distance from the cathode, whereas the electron saturation current  $I_e^*$  [defined here as  $I_e^* = I_e(I_p = +100 \text{ V})$ ] first increases rapidly and remains then nearly constant. From these data the electron temperature  $T_e$ , the electron density  $n_e$ , and

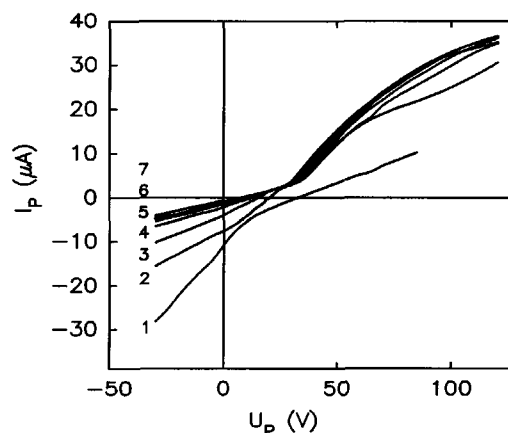


**Figure 2** Langmuir probe characteristics of the nitrogen plasma at different probe positions [distance probe–cathode:  $x$  = (curve 1) 2 cm, (2) 4 cm, (3) 6 cm, (4) 8 cm, (5) 10 cm, (6) 12 cm, and (7) 14 cm].

the ion density  $n_i$  were estimated according to the Langmuir theory using the following equations<sup>2</sup>

$$\frac{d \ln I_p}{dU_p} = - \frac{e}{kT_e} \quad (1)$$

$$n_e = \frac{I_e^*}{Se(kT_e/2\pi m_e)^{1/2}} \quad (2)$$

$$n_i = \frac{I_i^*}{0.6Se(kT_e/m_i)^{1/2}} \quad (3)$$

where  $m_e$  is the electron mass and  $m_i$  the ion mass (taken here for  $N_2^+$ ). Actually, eqs. (1)–(3) are valid only in the quasineutral plasma zone proposing a Maxwellian distribution of the velocity of the electrons and the ions. Analyzing the second derivative  $d^2 I_p/dU_p^2$  vs.  $U_p$  we found the Maxwellian electron energy distribution function to be a good approximation. So we assume to get at least meaningful tentative information about the main internal plasma parameters.

The results are summarized in Table I. They suggest extremely weak plasma conditions characterized by a low electron density nearly independent of the distance from the cathode. As it was proposed, the ion density is much higher (up to about two orders of magnitude at a distance of 2 cm behind the cathode). Thus, plasma conditions are realized at which reactions of the polymer surface with plasma gas specific cations (mainly  $N_2^+$ )<sup>3</sup> are in favor of the unspecific reactions initiated by energetic electrons.

To estimate the relative concentration of the neutral plasma species at different sample positions, the plasma emission line at 656.5 nm (representing the recombination of atomic nitrogen) was measured in dependence on the distance behind the cathode. Figure 3 shows the concentration gradient of the

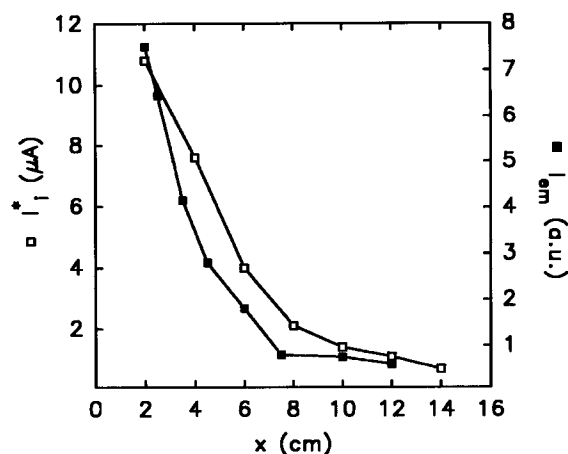


**Figure 3** Ion saturation current ( $I_i^*$ ) and emission intensity at 656.5 nm ( $I_{em}$ ) in dependence on the distance from the cathode ( $x$ ).

neutral plasma species is quite similar to that of the cations. These measurements do not provide, however, any information about the plasma radiation in the vacuum UV range.

### Sample Treatment and Contact-Angle Measurements

The changes at the sample surface during the plasma treatment at different positions behind the cathode were detected immediately after the treatment by contact-angle goniometry.

The dependence of the advancing and the receding contact angles with three test liquids on the treatment time for the sample position nearest to the cathode is shown in Figure 4. The receding contact angle, which mainly represents the modified (higher energetic) part of the sample surface, decreases rapidly with treatment time, whereas the advancing contact angle, which mainly represents the unmodified (low energetic) polymer surface, behaves smoothly except for a sharp decrease during the first 30 s. The difference between the advancing and the receding contact angles is shown in more detail in Figure 5. The hysteresis of about 20° for all three liquids in the case of the untreated sample is caused by the roughness of the polymer surface. Since electron microscopy does not show significant differences in the surface roughness of the untreated and the plasma-treated films, the sharp increase of the hysteresis during plasma treatment indicates an increasing chemical heterogeneity.

The high values up to about 60° for the hysteresis are somewhat surprising because they indicate either the formation of clusters of functional groups or, if

**Table I** Mean Electron Temperature ( $T_e$ ), Electron Density ( $n_e$ ), and Relative Ion Density ( $n_i/n_e$ ) Dependent on the Distance From the Cathode ( $x$ )

$x$ (cm)	$T_e$ (eV)	$n_e \cdot 10^{11}$ ( $m^{-3}$ )	$n_i/n_e$
2	—	—	124
4	3.0	1.5	46
6	2.7	1.6	19
8	2.1	1.6	10
10	3.0	1.3	6
12	2.3	1.7	5
14	2.5	1.5	4

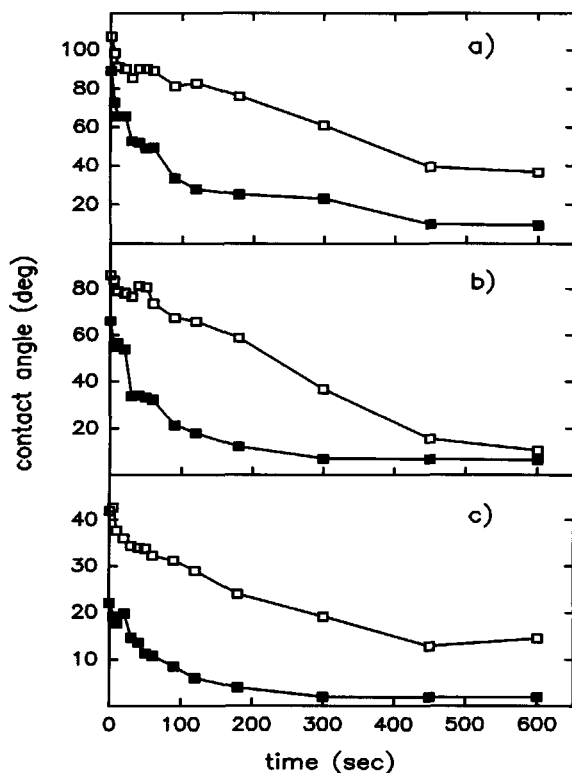


**Figure 4** (□) Advancing and (■) receding contact angles with three test liquids: (a) water; (b) formamide; and (c) tricresylphosphate in dependence on treatment time (nitrogen plasma,  $x = 2$  cm).

a random functionalization of the surface is assumed, a considerably higher lateral sensitivity of the contact angle measurements than is expected in the literature (about 100 nm).<sup>4</sup>

More information could be drawn from contact-angle data relating them to the surface free energy of the solid  $\gamma_s^{\text{tot}}$  and the test liquid  $\gamma_l^{\text{tot}}$  using Young's equation and one of the models assuming an additivity of different molecular interactions that determine the surface energy.<sup>5</sup> The interpretation of the experimental data is, however, complicated by the right choice of the model to be used. We shall discuss this problem in more detail elsewhere,<sup>6</sup> particularly based on the experimental data presented here. Meaningful values for the surface-free energy of the polymer solid were only derived considering the Lifshitz-van der Waals (LW) and the acid-base (AB) interactions as proposed by van Oss et al.<sup>7</sup>

$$\gamma_i^{\text{tot}} = \gamma_i^{\text{LW}} + \gamma_i^{\text{AB}} \quad (4)$$

$$\gamma_i^{\text{AB}} = 2(\gamma_i^{\ominus} \gamma_i^{\oplus})^{1/2} \quad (5)$$

where  $\gamma_i^{\ominus}$  stands for the electron acceptor (Lewis acid) part of the surface free energy of the compound  $i$ , and  $\gamma_i^{\oplus}$  for its electron donor (Lewis base) part

( $i = s, l$ ). Young's equation in terms of the LW-AB model can now be established

$$(1 + \cos \theta) \gamma_i^{\text{tot}} = 2[(\gamma_s^{\text{LW}} \gamma_l^{\text{LW}})^{1/2} + (\gamma_s^{\ominus} \gamma_l^{\oplus})^{1/2} + (\gamma_s^{\oplus} \gamma_l^{\ominus})^{1/2}]. \quad (6)$$

Measuring the contact angle of three test liquids with known parameters  $\gamma_i^{\text{LW}}$ ,  $\gamma_i^{\oplus}$ , and  $\gamma_i^{\ominus}$  (see Table II), we were able to calculate the three unknown parameters  $\gamma_s^{\text{LW}}$ ,  $\gamma_s^{\oplus}$ , and  $\gamma_s^{\ominus}$ . The results of such calculations for the experimental data represented in Figure 4 are shown in Figure 6.

The complex character of the chemical processes proceeding at the polymer surface during plasma treatment is demonstrated by different stages of the time dependence of the surface free energy and its components (Figure 6). During the first 30 s only functional groups acting as electron donors are formed, such as amines (considering only nitrogen containing groups; about the influence of oxygen see below) followed by a sharp increase of an electron-acceptor interaction. After 60 s this first main stage of the plasma/polymer interaction is achieved. However, it does not mean a complete functionalization of the polymer surface at all, as the high advancing contact angles and the great hysteresis indicate.

The state of complete modification is reached only at a treatment time of about 450 s and it is characterized by a total surface free energy of the polymer of about 58 mJ/m<sup>2</sup> as calculated from both the advancing as well as the receding contact angles. The increase of the total surface free energy of 31 mJ/m<sup>2</sup> for the untreated sample is mainly caused

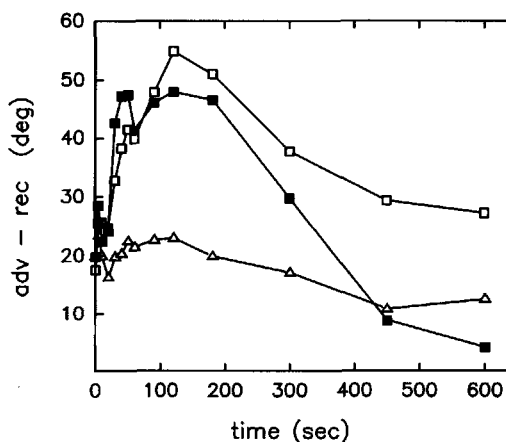


**Figure 5** Difference between the advancing and the receding contact angles with the three test liquids: (□) water; (■) formamide; and (△) tricresylphosphate in dependence on treatment time (nitrogen plasma,  $x = 2$  cm).

**Table II Surface Free Energy and Its Components in Terms of Eqs. (4) and (5) of the Three Test Liquids**

Test Liquid	$\gamma_i^{\text{tot}}$ (mJ/m <sup>2</sup> )	$\gamma_i^{\text{LW}}$ (mJ/m <sup>2</sup> )	$\gamma_i^{\ominus}$ (mJ/m <sup>2</sup> )	$\gamma_i^{\oplus}$ (mJ/m <sup>2</sup> )
Water <sup>a</sup>	72.8	21.7	25.5	25.5
Formamide <sup>b</sup>	57.4	32.0	3.0	52.9
TCP <sup>c</sup>	40.9	40.9	—	—

<sup>a</sup> Reference 15.

<sup>b</sup> Reference 15,  $\gamma^{\text{LW}}$  corrected by measurement in our laboratory,  $\gamma^{\ominus}$  and  $\gamma^{\oplus}$  were fitted keeping the ratio constant.

<sup>c</sup> Reference 14. Because of a lack of data the small polar surface free energy part reported in<sup>14</sup> (1.7 mJ/m<sup>2</sup>) was neglected and the LW was adjusted.

by an increase of the acid–base interactions and only to a minor extent by an increase of the Lifshitz–van der Waals interactions. Remarkably, the modified polymer surface acts as an electron donor as well as an electron acceptor.

Similar results, but with a different time scale and with less pronounced reaction stages, were obtained at the other sample positions investigated. The distance downstream from the cathode to the sample influences the formation of functional groups at the polymer surface only quantitatively but not qualitatively. The quantitative correlation is very

strong (Fig. 7), where the time scale of each curve is related to the ion saturation current at that sample position. Considering the information from the plasma diagnostics, especially the uniform concentration gradient of neutral as well as charged plasma species (Fig. 3), this result is not surprising indeed.

### Nitrogen, Oxygen, and Hydrogen Plasma— A Comparison

#### Plasma Diagnostics

In the case of the oxygen and the hydrogen plasmas, the plasma diagnostics were carried out in the same way as discussed above for the nitrogen plasma. As Figure 8 shows, the probe characteristics of the three plasma gases differs considerably. They indicate a very low concentration of cations in the case of the oxygen plasma and a high concentration of cations in the case of the hydrogen plasma. In both cases no electrons are detectable and the interpretation

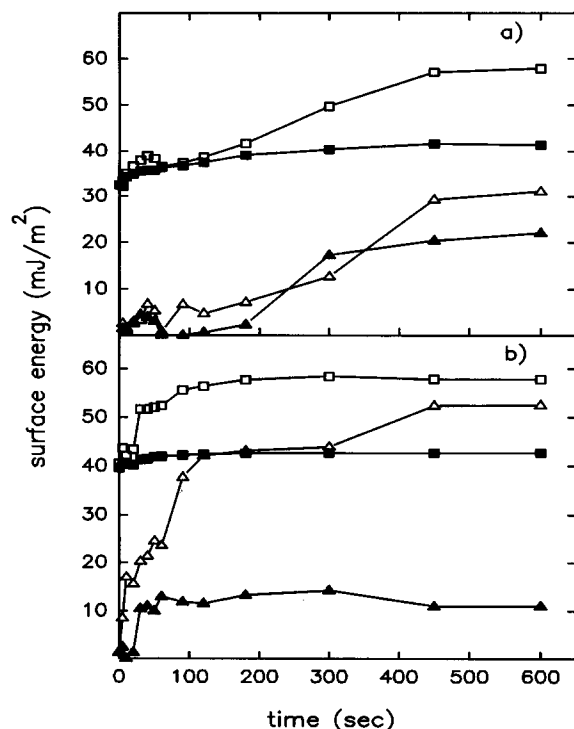


**Figure 6** (□) Total surface free energy of the polyethylene surface and its components (■)  $\gamma^{\text{LW}}$ , ( $\Delta$ )  $\gamma^{\ominus}$ , and ( $\blacktriangle$ )  $\gamma^{\oplus}$  calculated from (a) advancing and (b) receding contact angle in dependence on treatment time (nitrogen plasma,  $x = 2$  cm).

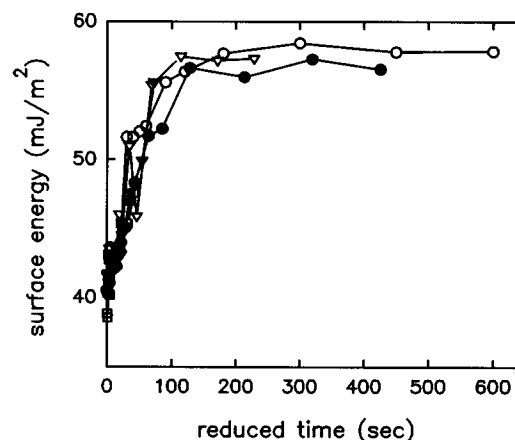


**Figure 7** Surface free energy of the polyethylene films plasma treated at different distances from the cathode in dependence on reduced treatment time  $t^* = t(I_{i,x}^*/I_{i,2}^*)$ .  $x =$  (○) 2 cm, (●) 4 cm, (▽) 6 cm, (▼) 10 cm, and (□) 14 cm.

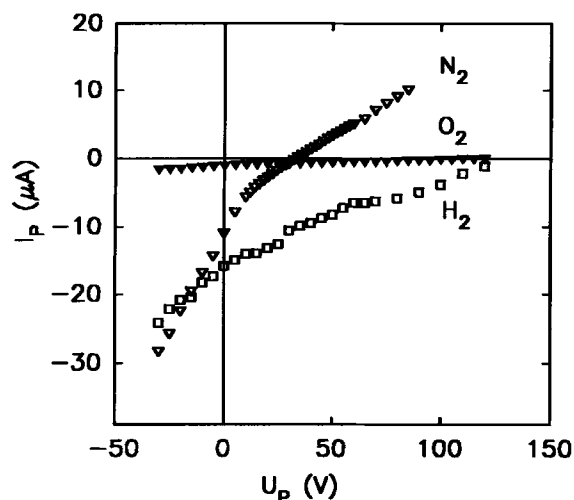


**Figure 8** Langmuir probe characteristics of the nitrogen, oxygen, and hydrogen plasmas (probe position  $x = 2$  cm).

of the experimental data in terms of eqs. (1)–(3) is therefore impossible.

**Sample Treatment and Contact-Angle Measurements**

The oxygen and the hydrogen plasma treatment were carried out for one sample position only ( $x = 2$

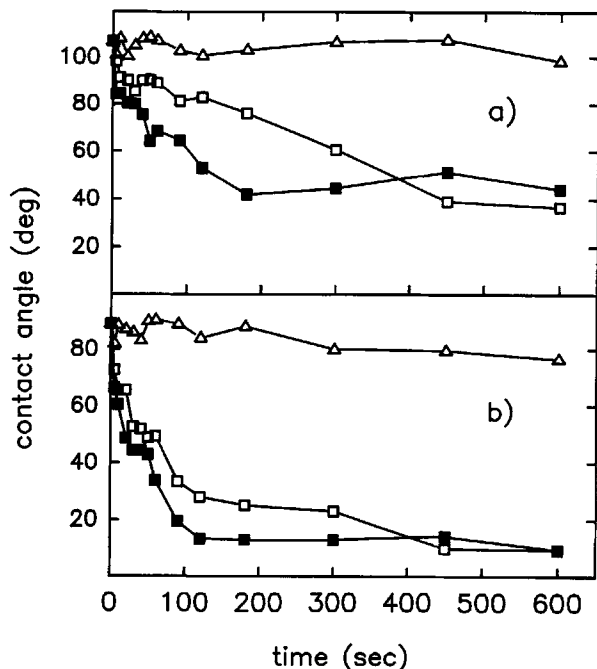


**Figure 9** (a) Advancing and (b) receding contact angle of water on polyethylene surfaces treated with (□) nitrogen, (■) oxygen, and (Δ) hydrogen plasmas in dependence on treatment time (sample position  $x = 2$  cm).

cm). The dependence of both the advancing and the receding contact angles on treatment time is very similar in the case of the oxygen plasma to that of the nitrogen plasma, whereas in the case of the hydrogen plasma only small changes are observed even after a long treatment time (Fig. 9). Contact-angle measurements with formamide and tricresylphosphate (TCP) as test liquids led to similar conclusions. The acid and the base components of the surface free energy (Fig. 10) underline the similarities in the behavior of the nitrogen and the oxygen plasma. The most pronounced difference is the rapid increase of the contents of functionalized groups acting as electron acceptors during the first 30 s of the oxygen plasma treatment. According to Gutmann's donor-acceptor approach<sup>8</sup> good electron acceptors are hydroxyl and carbon acid groups.

From Figures 9 and 10 it must be concluded that even in the case of the nitrogen plasma the functionalization of the polymer surface is mainly determined by oxygen traces in the plasma deriving

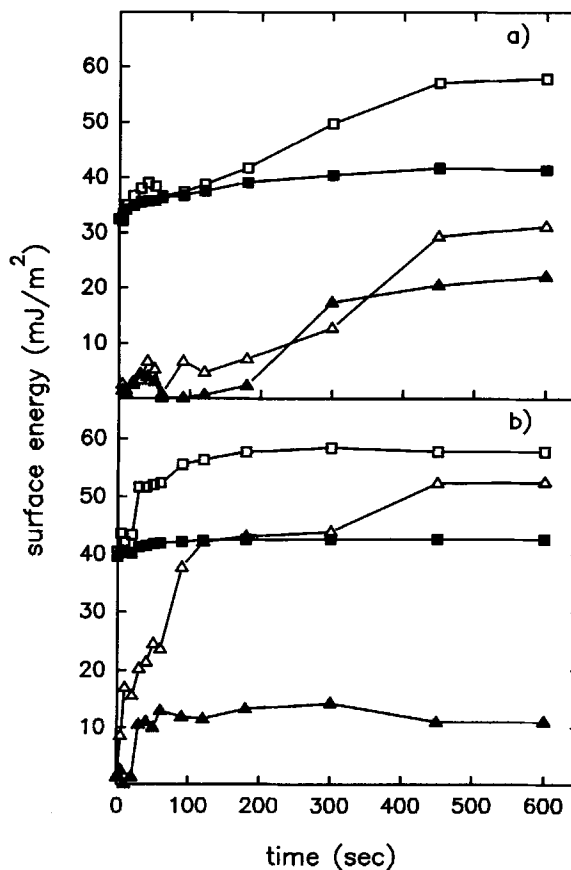


**Figure 10** (a) Acid and (b) base components of the surface free energy of polyethylene films treated with (□) nitrogen, (■) oxygen, and (Δ) hydrogen plasmas in dependence on treatment time (sample position  $x = 2$  cm).

from impurities of the nitrogen gas, from oxygen adsorbed by the sample and at the reactor walls, and from leakages in the vacuum system. A XPS-investigation of the sample treated 30 s in the nitrogen plasma at position  $x = 2$  cm confirms the conclusion drawn from contact-angle measurements: the quantitative analysis of the chemical composition of the polymer surface shows only a small amount of nitrogen incorporation (about 1%), but 5.2% oxygen content. The influence of oxygen residues during plasma treatment with inert gases is documented in the literature.<sup>1</sup> However, the fact that the nitrogen plasma under the specific experimental conditions used in the present work behaves rather like an oxygen plasma contaminated by nitrogen was unexpected, but may be understood in terms of the classical kinetic theory of gas. According to this theory the number of gas molecules  $z$  striking a unit area per second is given by<sup>9</sup>

$$z = \frac{N_A}{(2\pi R10^{-3})^{1/2}} \frac{p}{(TM)^{1/2}}, \quad (7)$$

where  $N_A$  is Avogadro's number,  $R$  the gas constant,  $p$  the pressure,  $T$  the absolute temperature, and  $M$  the molecular weight of the gas.

Using eq. (7) the collision rate of oxygen molecules deriving from air leakages at a basic pressure of 2 Pa in our plasma reactor at 300 K is about  $1 \cdot 10^{18} \text{ cm}^{-2} \text{ s}^{-1}$  compared to about  $1 \cdot 10^{20} \text{ cm}^{-2} \text{ s}^{-1}$  for the nitrogen molecules at the working pressure of 40 Pa. Thus, the collision rates differ only about two orders of magnitude, a difference that easily may be compensated by a higher crosssection for the reactions of oxygen plasma species (mainly atomic oxygen and molecular singlet oxygen)<sup>10,11</sup> with the polymer surface and by the fact that molecular oxygen is reactive toward polymeric alkyl radicals formed during plasma treatment. Moreover, the collision rate of about  $1 \cdot 10^{18} \text{ cm}^{-2} \text{ s}^{-1}$  must be compared with the number of monomeric units at the polymer surface, which may be roughly estimated to  $10^{15}$  per  $\text{cm}^2$ . Thus, there should be enough reactive oxygen in the nitrogen plasma to cover the polymer surface in a time scale of seconds or so.

With the background of these estimations it becomes obvious why extreme care has to be taken to get exclusively nitrogen containing functional groups while treating with a nitrogen plasma. Gerenser<sup>12</sup> attained such conditions using the chamber of an XPS instrument. In this case the basic pressure was  $6.7 \cdot 10^{-7}$  Pa ( $5 \cdot 10^{-9}$  Torr) and the collision rate of oxygen molecules with the sample surface is about  $4 \cdot 10^{11} \text{ cm}^{-2} \text{ s}^{-1}$ , e.g., several

orders of magnitude lower than the number of monomeric units at the polymer surface.

Similar effects of oxygen traces (though they are present) are not observed for the hydrogen plasma. In a more detailed investigation<sup>13</sup> we were able to show that in the case of a hydrogen plasma a higher oxygen content (above 0.1%) is necessary to give measurable effects on the contact angles. At a lower oxygen content the reactive oxygen species seem to be quenched by the hydrogen species; and/or oxygen-containing structures formed at the polymer surface are hydrogenated.

## CONCLUSION

Downstream behind the cathode of a dc glow discharge extremely weak plasma conditions are realized and the rate of the formation of functional groups at the polymer surface is controlled not by the kinetics of the plasma-polymer reactions but by the concentration of the plasma species at the sample surface. The time scale of the modification process (from tens to hundreds of seconds up to completion) allows the investigation of its main stages by the convenient characterization methods of polymer surfaces. In this paper contact-angle goniometry was used to obtain meaningful information about the changes at the surface of polyethylene during treatment in remote nitrogen, oxygen, and hydrogen plasmas.

In both the nitrogen as well as the oxygen plasma, a sharp increase of the chemical heterogeneity of the polymer surface was observed in a first reaction stage. The only difference is that in the case of the nitrogen plasma the heterogeneity is mainly caused by the formation of functional groups acting as electron acceptors, whereas in the case of the oxygen plasma during the first seconds of the plasma treatment a sharp increase in the content of electron-donor as well as electron-acceptor groups is detected.

In a second main reaction stage the surface modification becomes complete, leading to nearly the same chemical composition at the polymer surface since it could be concluded from the identical values of the surface free energy and its components obtained after the treatment of the polyethylene in the nitrogen and in the oxygen plasma.

The great similarity of the time dependence of the contact-angle data in the case of nitrogen and in the case of oxygen plasma clearly indicates a determining influence of oxygen residues in the plasma reactor for the nitrogen. According to the results of the plasma diagnostics, the observed effect is caused

by highly reactive neutral oxygen species, mainly molecular singlet oxygen.

The absence of such an effect in the case of the hydrogen plasma could result from direct quenching of reactive oxygen species and/or the chemical reduction of formed oxygen containing functionalities by hydrogen species.

The authors would like to thank Dr. Hantsche from Bundesanstalt für Materialforschung, Berlin, for recording XPS spectra.

## REFERENCES

1. R. Foerch, N. S. McIntyre, R. N. S. Sodhi, and D. H. Hunter, *J. Appl. Polym. Sci.*, **40**, 1903 (1990).
2. N. Hershkowitz, in *Plasma Diagnostics*, O. Anciello and D. L. Flamm, Eds., Academic Press, Boston and New York, 1989, p. 113.
3. S. Kumar and P. K. Ghosh, *Chem. Phys. Letters*, **179**, 463 (1991).
4. M. Yekta-Fard and A. B. Ponter, *J. Adhesion Sci. Technol.*, **6**, 253 (1992).
5. A. W. Adamson, *Physical Chemistry of Surfaces*, Wiley, New York 1990, p. 385.
6. A. Holländer, J. Behnisch, and H. Zimmermann, to appear.
7. C. J. van Oss, R. J. Good, and M. K. Chaudhury, *Langmuir*, **4**, 884 (1988).
8. V. Gutmann, *The Donor-Acceptor Approach to Molecular Interactions*, Plenum Press, New York and London, 1978.
9. W. J. Moore and D. O. Hummel, *Physikalische Chemie*, Walter de Gruyter, Berlin and New York, 1986.
10. A. Granier, S. Pasquiers, C. Boisse-Laporte, R. Darchicourt, P. Leprince, and J. Marec, *J. Phys. D: Appl. Phys.*, **22**, 1487 (1989).
11. F. Normand, J. Marec, P. Leprince, and A. Granier, *Mater. Sci. Eng.*, **A139**, 103 (1991).
12. L. J. Gerenser, *J. Adhesion Sci. Tech.*, **1**, 303 (1987).
13. A. Holländer, J. Behnisch, and H. Zimmermann, to appear.
14. F. M. Fowkes, *Ind. Eng. Chem.*, **56/12**, 40 (1964).
15. C. J. van Oss, L. Ju, M. K. Chaudhury, and R. J. Good, *J. Colloid Interface Sci.*, **128**, 313 (1989).

Received August 31, 1992

Accepted October 20, 1992